

REPORT DOCUMENTATION PAGE			Form Approved OMB NO. 0704-0188		
<p>The public reporting burden for this collection of information is estimated to average 1 hour per response, including the time for reviewing instructions, searching existing data sources, gathering and maintaining the data needed, and completing and reviewing the collection of information. Send comments regarding this burden estimate or any other aspect of this collection of information, including suggestions for reducing this burden, to Washington Headquarters Services, Directorate for Information Operations and Reports, 1215 Jefferson Davis Highway, Suite 1204, Arlington VA, 22202-4302. Respondents should be aware that notwithstanding any other provision of law, no person shall be subject to any penalty for failing to comply with a collection of information if it does not display a currently valid OMB control number. PLEASE DO NOT RETURN YOUR FORM TO THE ABOVE ADDRESS.</p>					
1. REPORT DATE (DD-MM-YYYY) 12-12-2016		2. REPORT TYPE Final Report		3. DATES COVERED (From - To) 23-Nov-2015 - 22-Aug-2016	
4. TITLE AND SUBTITLE Final Report: STIR: Ignition by Electric Spark Discharges Triggered by the Fuel/Energetic Aerosol Itself			5a. CONTRACT NUMBER W911NF-16-1-0015		
			5b. GRANT NUMBER		
			5c. PROGRAM ELEMENT NUMBER 611102		
6. AUTHORS Stephen Tse			5d. PROJECT NUMBER		
			5e. TASK NUMBER		
			5f. WORK UNIT NUMBER		
7. PERFORMING ORGANIZATION NAMES AND ADDRESSES Rutgers, The State University of New Jersey 3 Rutgers Plaza ASB III, 2nd Floor New Brunswick, NJ 08901 -8559			8. PERFORMING ORGANIZATION REPORT NUMBER		
9. SPONSORING/MONITORING AGENCY NAME(S) AND ADDRESS (ES) U.S. Army Research Office P.O. Box 12211 Research Triangle Park, NC 27709-2211			10. SPONSOR/MONITOR'S ACRONYM(S) ARO		
			11. SPONSOR/MONITOR'S REPORT NUMBER(S) 68129-EG-II.1		
12. DISTRIBUTION AVAILABILITY STATEMENT Approved for Public Release; Distribution Unlimited					
13. SUPPLEMENTARY NOTES The views, opinions and/or findings contained in this report are those of the author(s) and should not be construed as an official Department of the Army position, policy or decision, unless so designated by other documentation.					
14. ABSTRACT In this project, electric breakdown triggered by the presence of non-conductive droplets is studied with experiment and simulation. The presence of droplets can lower the threshold for breakdown by a large extent. There are several modes to trigger spark by the presence of droplets: (1) electrospray from the deposited liquid on the electrode; (2) single droplet repelled from the deposited liquid moving toward the opposite electrode; (3) single droplet attracted to an electrode but then forming an electrospray; and (4) presence of a single droplet very close to an electrode. The mechanism for triggering of the spark is attributed to electric field enhanced by the presence of high dielectric					
15. SUBJECT TERMS Aerosol, ignition, electric spark					
16. SECURITY CLASSIFICATION OF:		17. LIMITATION OF ABSTRACT		15. NUMBER OF PAGES	19a. NAME OF RESPONSIBLE PERSON
a. REPORT UU	b. ABSTRACT UU	c. THIS PAGE UU	UU		Stephen Tse
				19b. TELEPHONE NUMBER 848-445-0449	

Report Title

Final Report: STIR: Ignition by Electric Spark Discharges Triggered by the Fuel/Energetic Aerosol Itself

ABSTRACT

In this project, electric breakdown triggered by the presence of non-conductive droplets is studied with experiment and simulation. The presence of droplets can lower the threshold for breakdown by a large extent. There are several modes to trigger spark by the presence of droplets: (1) electrospray from the deposited liquid on the electrode; (2) single droplet repelled from the deposited liquid moving toward the opposite electrode; (3) single droplet attracted to an electrode but then forming an electrospray; and (4) presence of a single droplet very close to an electrode. The mechanism for triggering of the spark is attributed to electric field enhanced by the presence of high dielectric-constant liquid. The presence of materials in-between the electrode may also hinder the spark because of the adhesion of the initial ions onto the surfaces of the droplets or particles.

Enter List of papers submitted or published that acknowledge ARO support from the start of the project to the date of this printing. List the papers, including journal references, in the following categories:

(a) Papers published in peer-reviewed journals (N/A for none)

<u>Received</u>	<u>Paper</u>
-----------------	--------------

TOTAL:

Number of Papers published in peer-reviewed journals:

(b) Papers published in non-peer-reviewed journals (N/A for none)

<u>Received</u>	<u>Paper</u>
-----------------	--------------

TOTAL:

Number of Papers published in non peer-reviewed journals:

(c) Presentations

Number of Presentations: 0.00

Non Peer-Reviewed Conference Proceeding publications (other than abstracts):

Received Paper

TOTAL:

Number of Non Peer-Reviewed Conference Proceeding publications (other than abstracts):

Peer-Reviewed Conference Proceeding publications (other than abstracts):

Received Paper

TOTAL:

Number of Peer-Reviewed Conference Proceeding publications (other than abstracts):

(d) Manuscripts

Received Paper

TOTAL:

Number of Manuscripts:

Books

Received Book

TOTAL:

Received

Book Chapter

TOTAL:

Patents Submitted

Patents Awarded

Awards

Graduate Students

<u>NAME</u>	<u>PERCENT SUPPORTED</u>
FTE Equivalent:	
Total Number:	

Names of Post Doctorates

<u>NAME</u>	<u>PERCENT SUPPORTED</u>
Zhizhong Dong	0.50
Gang Xiong	0.50
FTE Equivalent:	1.00
Total Number:	2

Names of Faculty Supported

<u>NAME</u>	<u>PERCENT SUPPORTED</u>
FTE Equivalent:	
Total Number:	

Names of Under Graduate students supported

<u>NAME</u>	<u>PERCENT SUPPORTED</u>
FTE Equivalent:	
Total Number:	

Student Metrics

This section only applies to graduating undergraduates supported by this agreement in this reporting period

The number of undergraduates funded by this agreement who graduated during this period: 0.00

The number of undergraduates funded by this agreement who graduated during this period with a degree in science, mathematics, engineering, or technology fields:..... 0.00

The number of undergraduates funded by your agreement who graduated during this period and will continue to pursue a graduate or Ph.D. degree in science, mathematics, engineering, or technology fields:..... 0.00

Number of graduating undergraduates who achieved a 3.5 GPA to 4.0 (4.0 max scale):..... 0.00

Number of graduating undergraduates funded by a DoD funded Center of Excellence grant for Education, Research and Engineering:..... 0.00

The number of undergraduates funded by your agreement who graduated during this period and intend to work for the Department of Defense 0.00

The number of undergraduates funded by your agreement who graduated during this period and will receive scholarships or fellowships for further studies in science, mathematics, engineering or technology fields:..... 0.00

Names of Personnel receiving masters degrees

NAME
Total Number:

Names of personnel receiving PHDs

NAME
Total Number:

Names of other research staff

NAME PERCENT SUPPORTED
FTE Equivalent:
Total Number:

Sub Contractors (DD882)

Inventions (DD882)

Scientific Progress

See Attachment.

Technology Transfer

STIR: Ignition by Electric Spark Discharges Triggered by the Fuel/Energetic Aerosol Itself

(Grant W911NF-16-1-0015)

Final Report

PI: Stephen D. Tse, Rutgers University

1 Introduction

Electric spark is commonly used for ignition of flame-based systems, however, unwanted sparks may cause a major safety concern in combustible environments [1] and in gas insulated systems [2]. Electric spark discharge occurs when the gap between electrodes is bridged by some region of ionization path. Well controlled conditions are crucial for the application of electric spark.

The presence of droplets and particles are reported to disturb the electric field between the electrodes and alter the breakdown threshold for spark. Free particles have been found to be more harmful to the dielectric strength of an ionized air gap than the fixed conductive spheres located on the surface of an electrode [3]. In gas insulated systems, conducting particles have been shown to trigger spark and cause problems [2,4]. This effect has been simulated computationally, but only for conductive particles [5]. However, for non-conducting materials in the electric field, research has been limited to studying fibers in SF₆ gas gap [6]. The effect of non-conductive glycerol aerosol on the current-voltage curve of spark discharge was studied by Riebel et al. [7], with results showing that the effect of aerosol on the spark discharge is dependent on the size of the electrodes. The current-voltage curve was shifted to higher voltages with the introduction of aerosol for 0.2mm-diameter electrodes; however, the onset voltage for corona was reduced for 2mm-diameter electrodes. Stommel et al. [8] further investigated the spark triggered by glycerol droplets and found a thorn of liquid at the tip of an electrode pointing at the opposite electrode. The strong curvature of the thorn was claimed to be working as a sharpened electrode and shift the onset voltage to lower values. Randeberg et al. [1] found that dust itself can initiate electric spark discharge, causing subsequent dust explosion. Large particles were found to trigger the spark at lower voltages than do smaller ones. Nevertheless, the governing mechanisms for the initiation of spark are not well understood.

The fundamental mechanisms involved in electric spark triggered by droplets or particles need further investigation, for non-conducting fuels and liquids, as well as other parameters. In this project, the electric spark triggered by the presence of non-conductive droplets is investigated. Several different modes for triggering of the spark by the droplets are revealed by high-speed imaging. Computational simulation conducted with COMSOL also aids in understanding the effects of droplet presence, size, and composition on spark initiation.

2 Experimental setup:

A schematic of the setup is shown in Fig. 1. High voltage is applied across two 100- μm diameter tungsten electrodes, and droplets are sprayed in-between them. The tungsten electrodes are point-to-point, placed with a separation distance of 1 mm. The high voltage is supplied by a Bertan high voltage power supply, with external resistor and capacitor to control the spark frequency. For preliminary testing, commercial CRC Brakleen Brake Parts Cleaner is sprayed in-between the electrodes. The composition listed for this solution is: methanol (40-50%), toluene (10-20%), acetone (5-15%), 3-methylhexane (5-10%), carbon dioxide (5-10%), n-heptane (5-10%), methylcyclohexane (3-5%), naphtha (3-5%), cyclohexane (1-3%), and ethylbenzene (<0.2%).

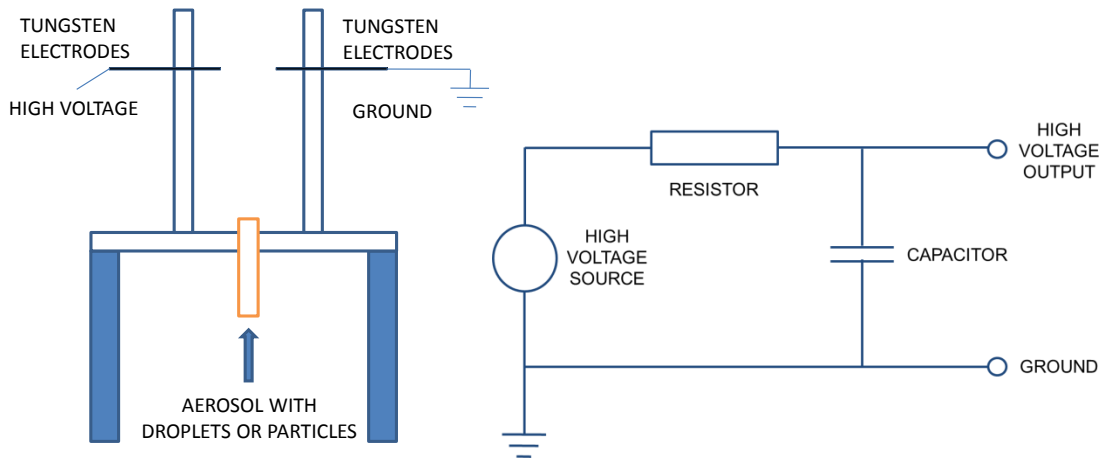


Fig. 1. Electrode wire-wire configuration for breakdown testing, with the right figure showing the high voltage power supply

A high speed camera (Phantom V2011) is employed for visualizing triggering of the electrical spark. The 12-bit depth high speed camera can go up to 1,000,000 fps, with resolution of 128×16 pixels, and up to 22,500 fps at full resolution of 1280×800 . A 300W Neon Arc lamp is utilized to illuminate the region of interest to provide enough light for the high speed camera to work at very low exposure time ($\sim 1 \mu\text{s}$). The sketch of the imaging system is shown in Fig. 2.

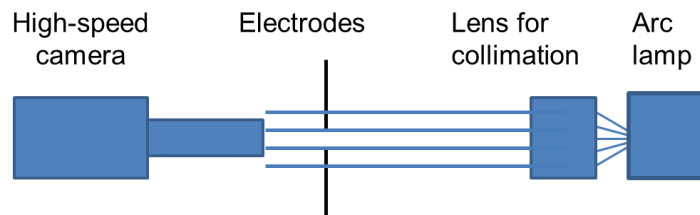


Fig. 2. Electrode wire-wire configuration for breakdown testing

For fundamental understanding of spark triggering by droplets, droplets of single component with controlled size and concentration are utilized in the research. Water, methanol, and toluene are tested for their ability to trigger spark discharge. The setup for droplets generation is shown in Fig. 3. An ultrasonic atomizer (Sono-Tek 8700-120) is employed to produce droplets from a liquid supply line, which is then controlled by a peristaltic pump. To better control the droplet concentration and the environment, a shield tube is aligned around the atomizer and gas flow with controlled flow rate, delivering a spray of droplets into the test area.

The droplets from the atomizer are first characterized with a CCD camera (SONY SX90), where the pixel size is $3.75\ \mu\text{m}$, much smaller than the high speed camera ($28\ \mu\text{m}$) to better identify the size information of the droplets. The images captured by the camera are then processed with Matlab to analyze the size of the droplets generated. Two examples of the identified droplets are shown in Fig. 4. The white spots on the left-side figure are the droplets, and red circles on the right-side figure are the droplets identified by Matlab. The results show good identification of droplet position and size.

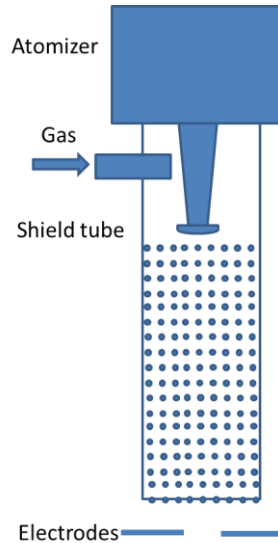


Fig. 3. Setup for droplets generation with controlled size and concentration.

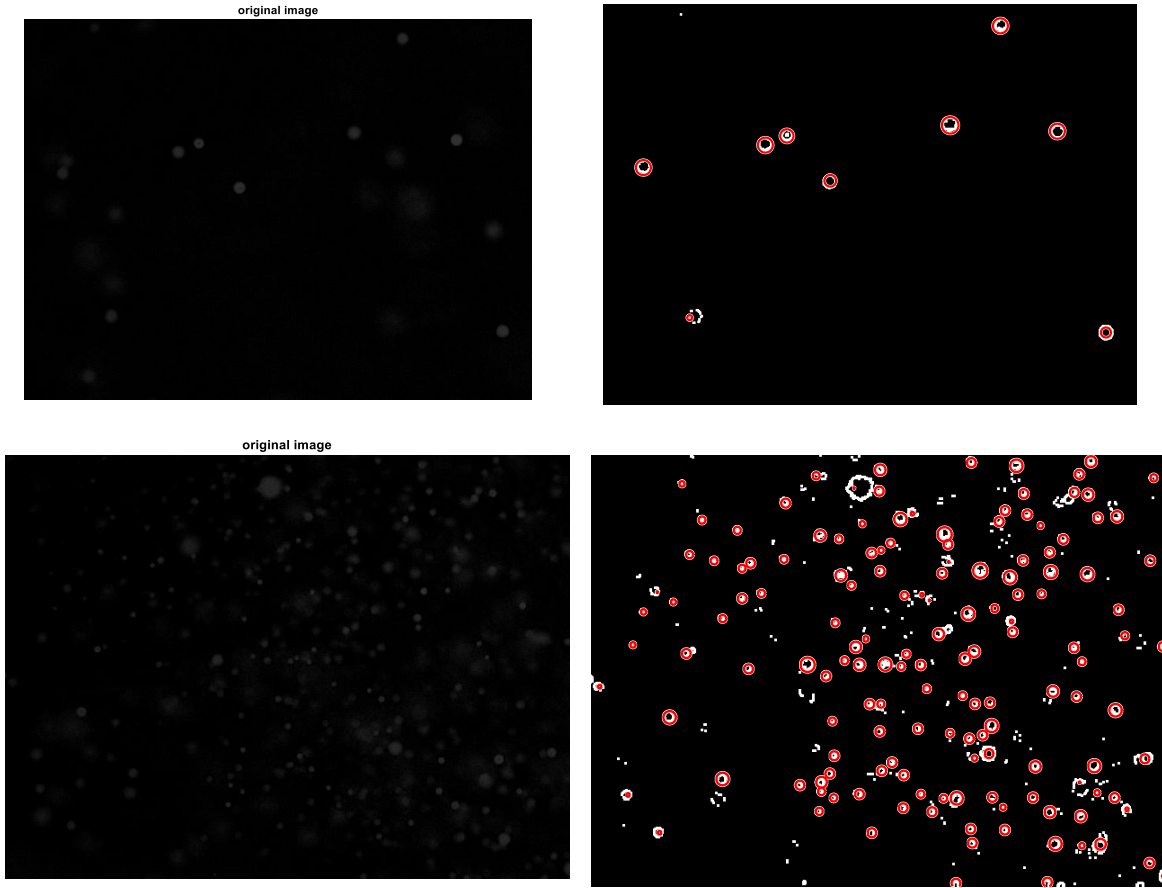


Fig. 4. Particle size identification with Matlab for two cases. Left: original image. Right: identified droplets.

The droplet size distribution of the water droplets is then fitted, with the result shown in Fig.5. The mean diameter of the droplets is $18\mu\text{m}$.

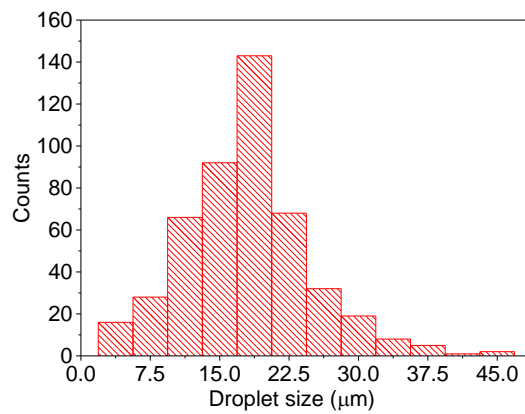


Fig. 5. Droplet size distribution from the atomizer.

3 Results and discussions:

3.1 Preliminary test with CRC spray

For the given setup, in air without the presence of droplets, the onset voltage for continuous spark is above 3,100V, and there is no spark at all at 3,000V. However, upon spraying the aerosol across the gap between the two electrodes, spark is initiated immediately, as seen by eye. With the high-speed camera capturing the detailed information before the spark, it is found that the liquid on the electrode forms a cone-like thorn on the tip of the ground (right) electrode, similar to that observed by Stommel et al. [8]. However, in our case, a very fine micro-electrospray (see circled region of Fig. 6) then emanates from this liquid thorn on the ground (right) electrode, spurting towards the +3,000V (left) electrode in the high-strength electric field. The spark is triggered soon after.

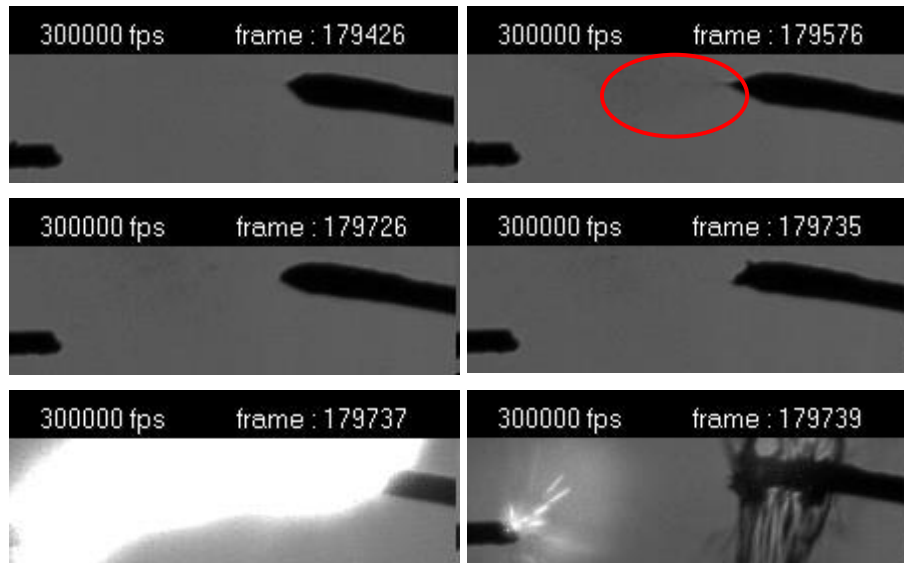


Fig. 6. High-speed images of induced breakdown at 3,000V.

To isolate the effect of liquid layer from the droplets in between the electrodes, the ground electrode (left) is pre-wetted with the CRC liquid before the high voltage bias is applied. At 2,500V, spark is triggered with the liquid layer, as shown in Fig. 7. A droplet forms from the liquid layer on the ground (right) electrode, and moves leftward, being pulled by the electric field. A liquid thorn tip on the high-voltage (left) electrode is formed, and the induced electrospray from the liquid film is circled in the second image (frame 595500); the same area is circled in the third image (frame 596400) for comparison. The large droplet on the right electrode actually proceeds to partially bridge the gap, forming an irregular globular shape. Breakdown occurs in frame 596422, encompassing liquid globules.

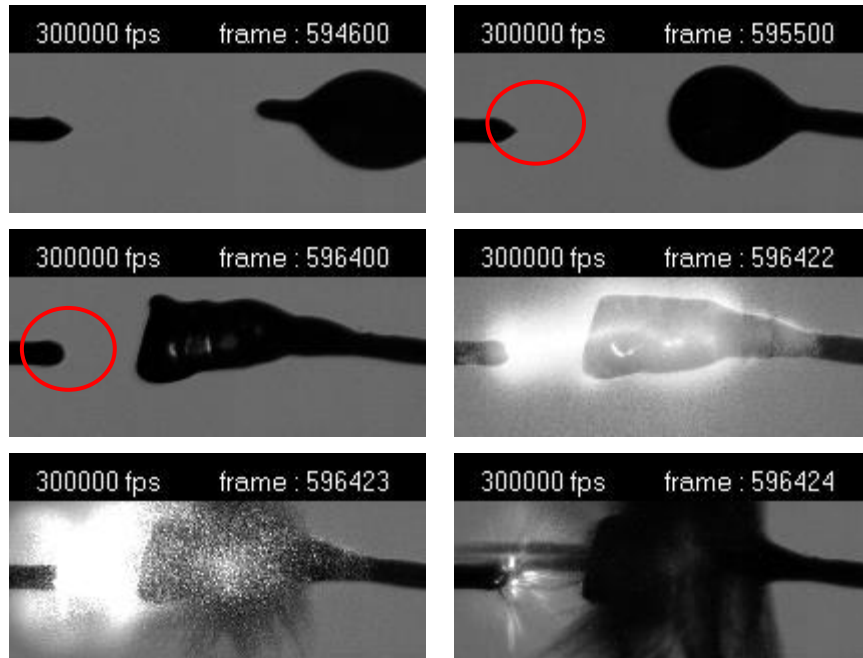


Fig. 7. Imaging of breakdown at 2,500V, with wetted ground (right) electrode.

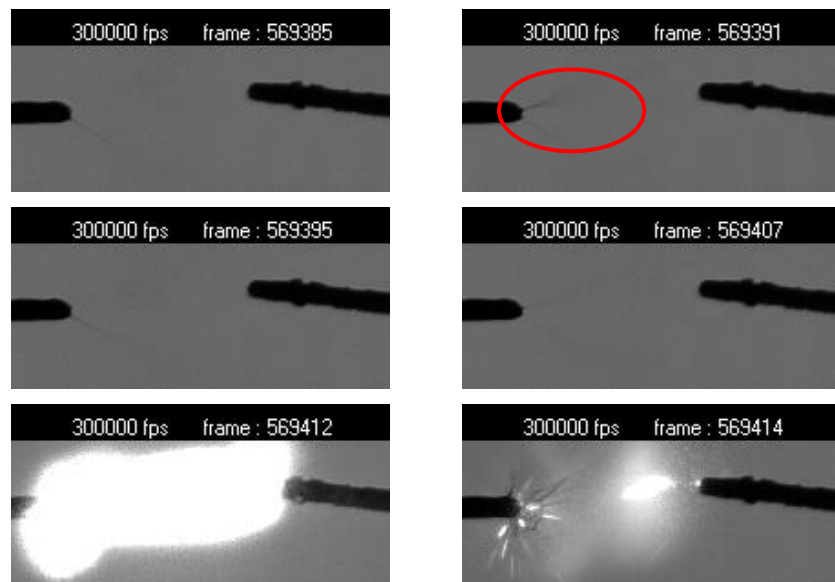


Fig. 8. Spark at 2,500V, with wetted high voltage wire (left) by electrospay.

To assess the role of polarity, the high voltage electrode (left) is pre-wetted with the CRC solution to study spark triggering. Upon application of high voltage of 2,500V, the high-speed camera captures the ensuing events, as shown in Fig. 8. An electrospay is seen emitting from the active electrode from the deposited liquid layer, as circled in the second image frame 569391, and the electrospay initiates the spark soon.

3.2 Triggered spark with single component

Droplets with single component and controlled size and concentration are then tested for a better fundamental understanding of the triggering of the spark. The voltage required to generate the spark between the two tungsten electrodes without droplets is about 3,100V, which can be decreased to about 2,300V with water droplets.

Besides the spark triggered by the electrospray, as seen in the CRC spray case, there are several more modes for droplets to trigger the spark. In one mode, one single droplet is ejected from one electrode to the other one, triggering the spark as the droplet gets close to the other electrode, as shown in Fig. 9. In this case, the water droplet triggers the spark at a voltage of 2,300V. One single droplet is formed (Img# 36900) from pulling the liquids from the electrode on the left side. As the droplet gets close to the electrode on the right side, the shape of the droplet changes much, as seen in Img# 36955, and then triggers the spark in the following Img# 36956. The frame rate of the high-speed camera is 301,075 fps. Thus the time interval between the images is only 3.3 μ s.

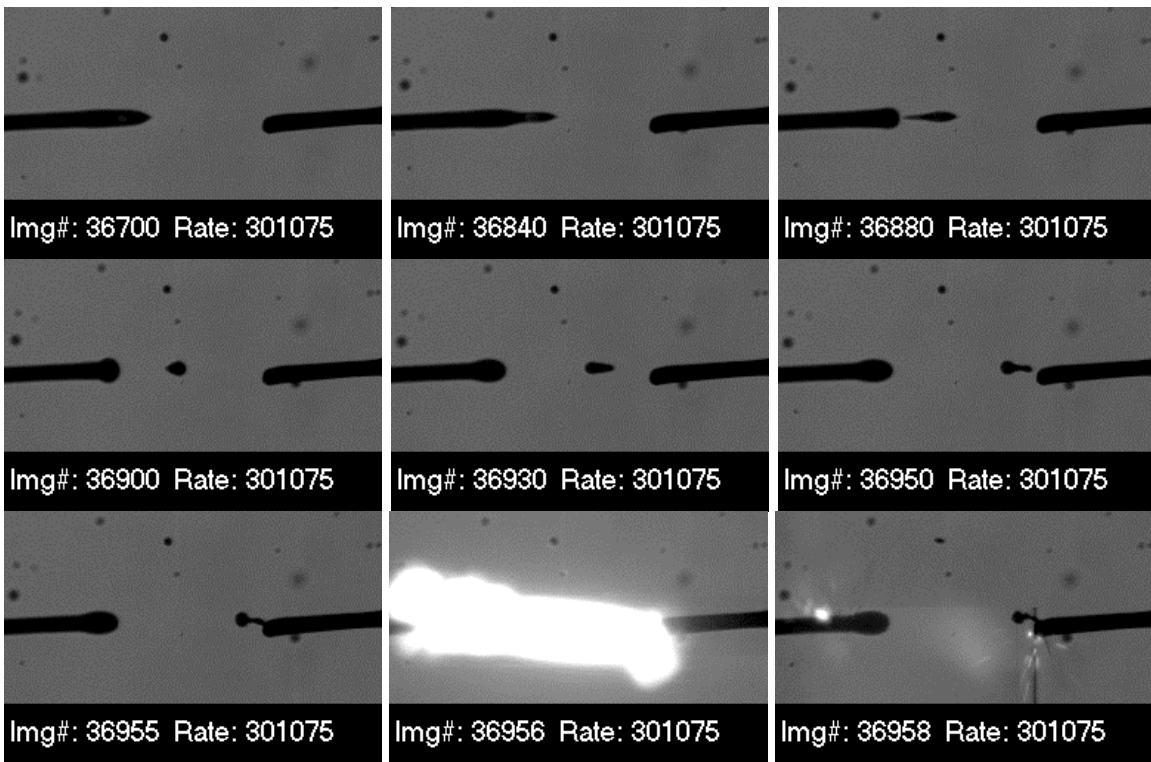


Fig. 9. Images of breakdown at 2,300V, with water droplets where one droplet ejects from an electrode, triggering spark.

In another mode, one small droplet gets close to one electrode, being attracted to it, but is then ejected away in the form of a fine spray, triggering the spark, as shown in Fig. 10. In Img# -721735, the small droplet gets close to the electrode. After attachment, the liquid is ejected from the electrode in Img#-721720, and the spark is triggered

thereafter in the following image. Since the jet of droplets can have guiding effect on streamer advancement [9], the ejection of droplets or electrospray can favor streamer propagation and thus spark across the electrodes.

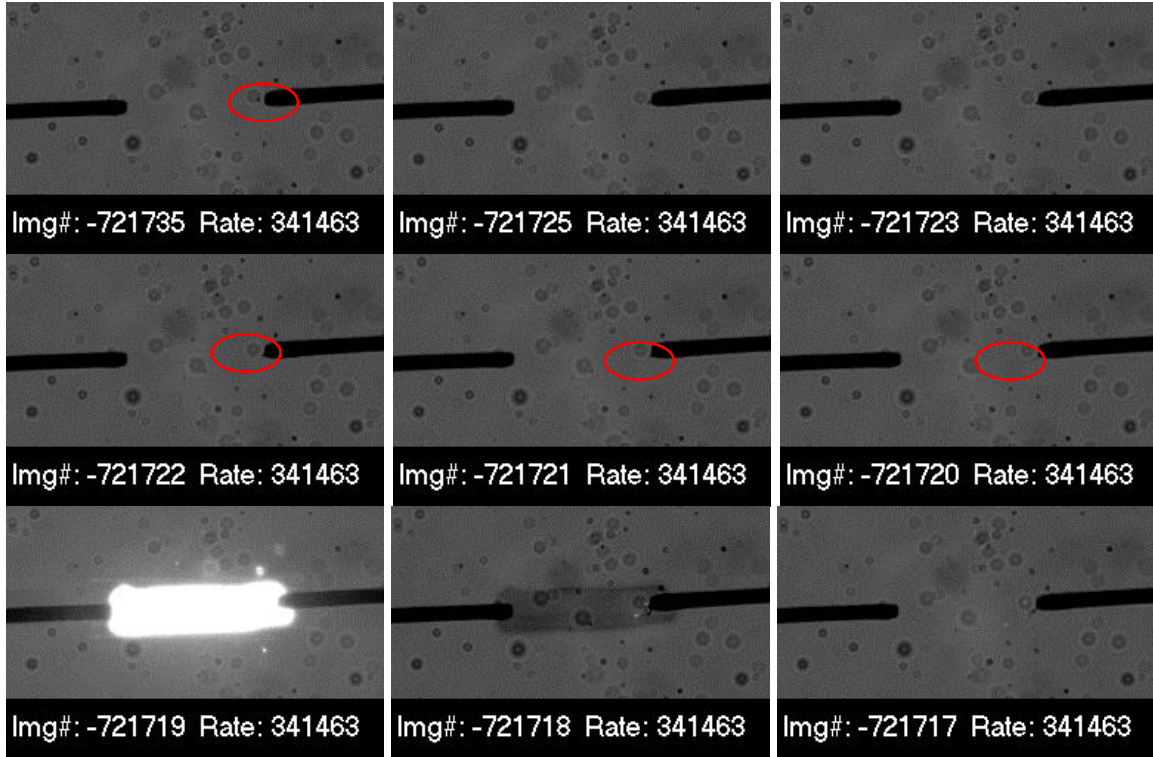


Fig. 10. Images of breakdown at 2,600V, with water droplets where liquid ejection from an electrode triggers spark.

There are also triggered sparks without the ejection of droplet or liquid when a droplet is present in the vicinity of an electrode, as shown in Fig. 11. One droplet is present close to the electrode, as shown in the red circle in Img# -700305. The droplet is then pulled to the electrode, and the shape of the droplet is changed, as some part of the droplet is pulled to the electrode, in Img# -700301 to Img#-700298. Then spark is initiated.

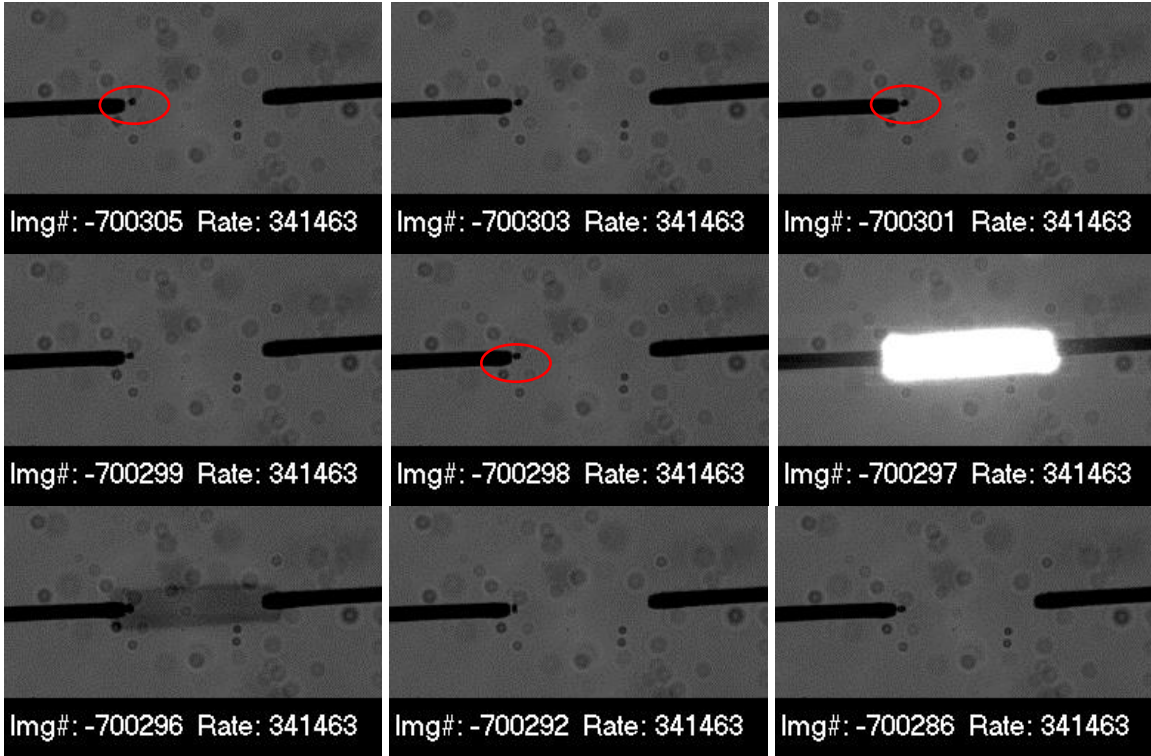


Fig. 11. Images of breakdown at 2,600V, with water droplet presence triggering spark.

3.3 Droplet movement close to the electrodes

The droplet movement is studied as the droplet approaches the electrode to understand the interaction of the droplet and electrode wire on the initiation of spark.

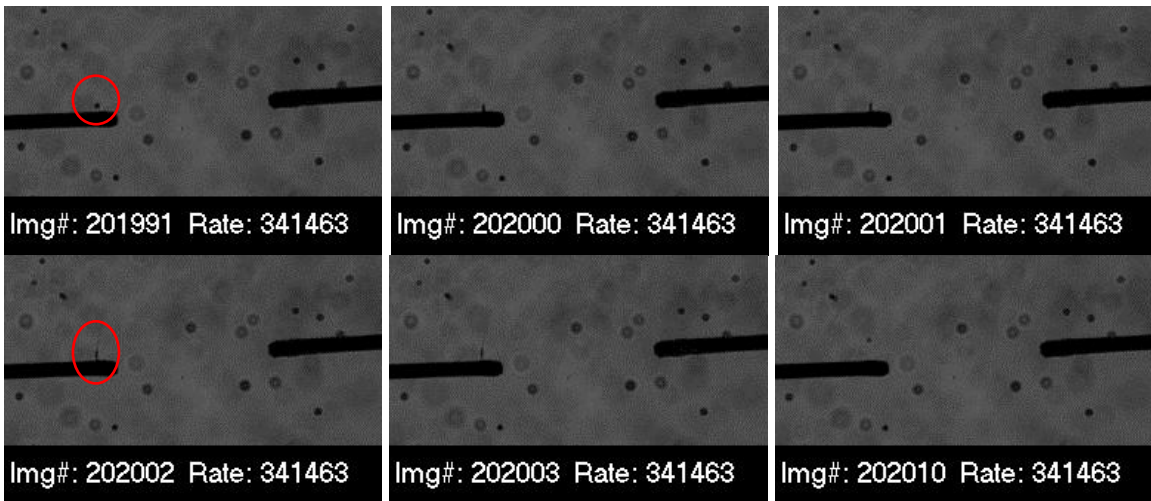


Fig. 12. Images of droplet movement close to the electrode under 3,000V (Type 1).

Two types of droplet movements are observed as it gets close to the electrodes. In Type 1, as shown in Fig. 12, as the droplet approaches the electrode, it is attracted by and attaches to the electrode; however, some part of liquid is then ejected away, as shown in Img#202002.

On the contrary, in Type 2, as shown in Fig. 13, the droplet is attracted to the electrode and stays there. It is worth noting that the Type 1 scenario occurs more often on the high positive voltage electrode (left wire), while Type 2 occurs more often on the ground wire (right wire).

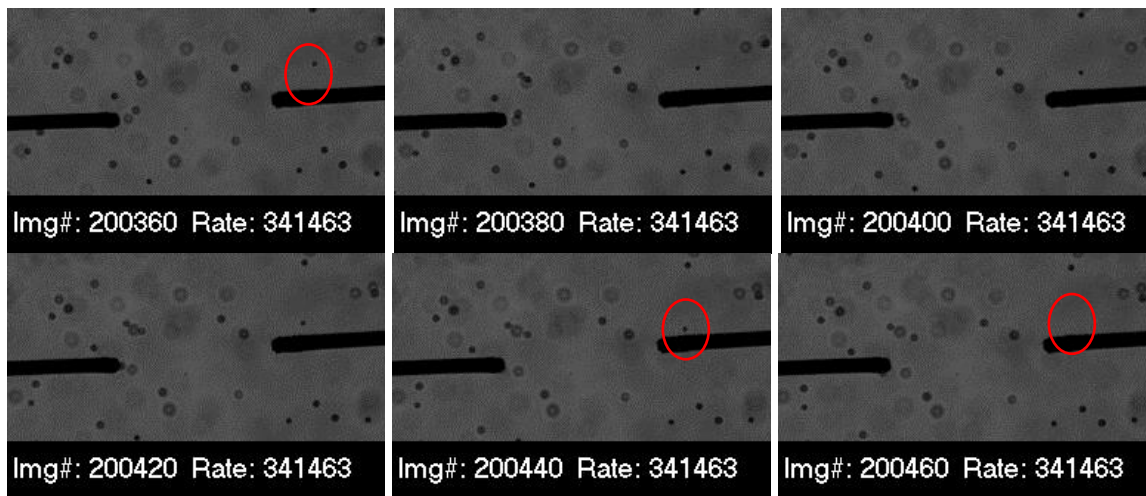


Fig. 13. Images of droplet movement close to electrode under 3,000V (Type 2).

In both types, before their attachment on the electrodes, the droplets are attracted by and accelerated to the electrode. However, after the deposition on the electrode, the liquid undergoes a process similar to the electrospray under high voltage [10,11], producing fine droplets with electrostatic charge. These charged droplets can be dispersed in between the two electrodes, changing the electric field and initiating spark.

3.4 Triggered spark with different droplets (methanol and toluene)

Other than water droplets, methanol and toluene droplets are also tested to investigate the effect of different liquids. For the experiments with methanol, the triggering behavior is similar to that for the water case. However, toluene behaves quite differently than do water and methanol. As the toluene droplet gets close to the electrode, it also experiences attraction, and can also be ejected away from the electrode after deposition, but no sparks are triggered. Two different cases imaging the movement of toluene droplets are shown in Fig. 13 and Fig. 14, with no sparks ensuing. Moreover, as there are some depositions of liquids on the wire, as shown in Fig. 14, it is even harder to break down than if there were air only. There is ejection occurring between the two electrodes, and the liquids are pulled closer to each other, but no breakdown, at 3600V. Such an event can even last for a few seconds at 5,000V before a large spark is triggered. This result indicates that spark

can either be triggered at a lower voltage or hindered at a higher voltage by the presence of droplets.

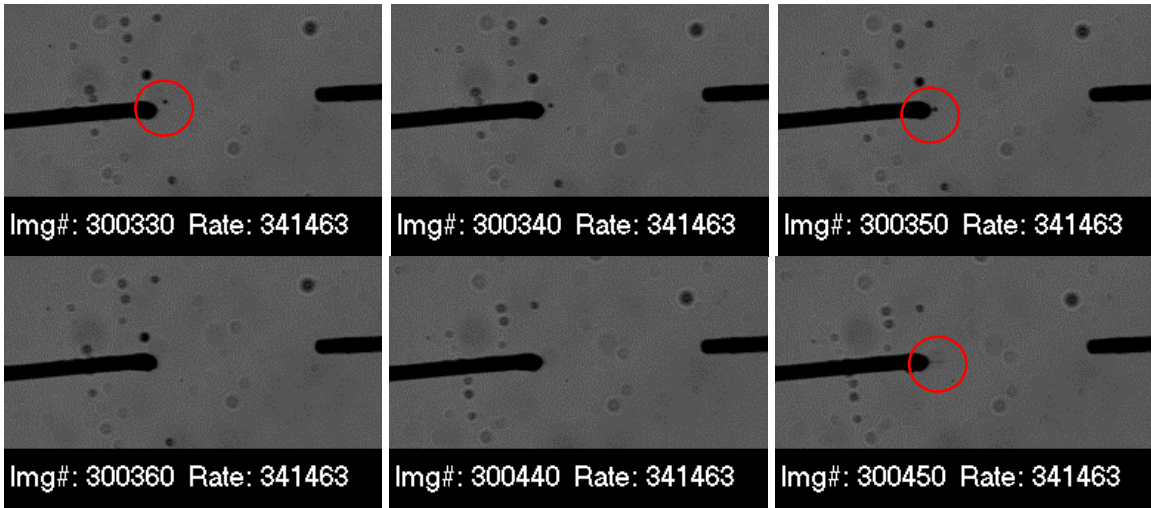


Fig. 13. Images of toluene droplet ejection after depositing on wire under 3,000V.

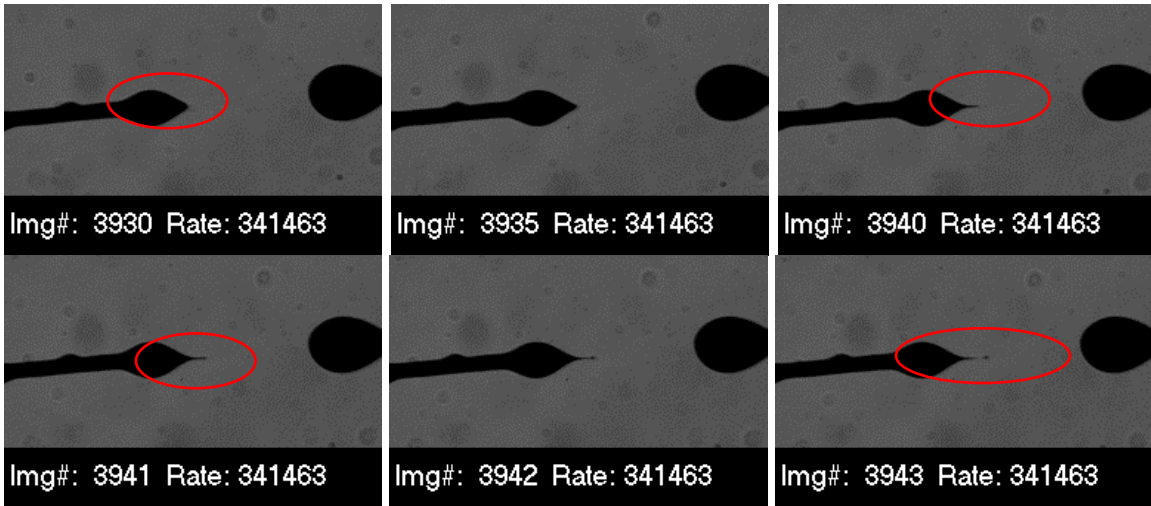


Fig. 14. Images of toluene droplet ejection from wire under 3,600V.

3.5 Triggered spark by solid fiber

The shape of the droplet is always changed as it approaches the electrode. For comparison and better understanding of the initiation of the spark, the effect of a non-deforming solid material on spark initiation is studied. A 125- μm size optical fiber is inserted in between the two electrodes. The results show that the threshold voltage for the spark cannot be decreased, no matter where the fiber is located, even when the fiber touches the electrode.

Another case is tested to check on the effect of the fiber on the spark. At high voltage above the threshold for spark, the spark will be continuously generated with the external high voltage power supply system, and the frequency is controlled by the external loop with the resistor and the capacitor because of the spark (discharge) and charging process (to the capacitor). Without the presence of the fiber, the interval between the sparks is about 160 frames with a 341,463 fps frame rate, leading to a spark frequency of about 2,100 Hz. However, as the fiber approaches the electrode, the interval between the sparks is increased, as shown in Fig. 15.

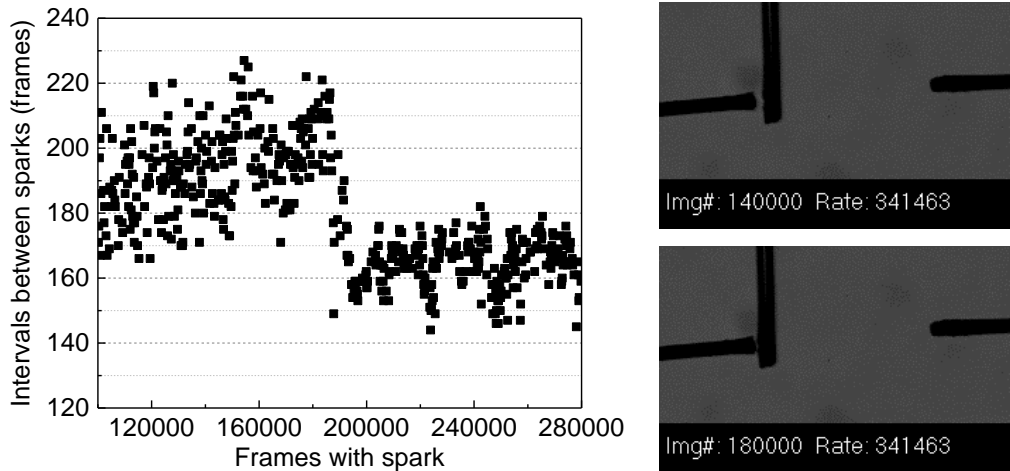


Fig. 15. Sparking in the presence of an optical fiber.

From frame 100000 to frame 180000, the distance between the fiber and the electrode is decreasing; however, it is more difficult to initiate a spark. Not until the fiber touches the electrode does spark initiation become easier than if there were no fiber. The presence of the optical fiber may block the path for initial ions to move from one electrode to another [12], thus hindering the initiation of spark. This effect may also play some role for the droplets to some extent.

3.6 COMSOL simulation and discussions

To understand the mechanisms for the triggering process, analysis and simulation are conducted. COMSOL software is employed to perform the electrostatics simulation of the potential and electric fields. The effect of the presence of droplet, the distance between the electrode and droplet, the size of droplet, and properties of the droplet are studied.

3.6.1 Electric field enhancement with droplet

A 3-dimensional domain of 12-mm diameter area with two 100 μm wire electrodes (high voltage wire at 3,000V and ground wire at 0V) is calculated to understand the effect of droplet presence. The electric field without droplet is shown in Fig. 16, with maximum electric field strength of $\sim 2.5 \times 10^7$ V/m. However, with a 20 μm water droplet 10 μm

away from electrode, the maximum electric field strength can be enhanced up to $\sim 5 \times 10^7$ V/m in between the left electrode and the droplet, as shown in Fig. 16. The maximum electric field strength on the right side of the droplet is also enhanced to 3.2×10^7 V/m. The initiation of the spark by the presence of the droplet is attributed to this enhanced electric field.

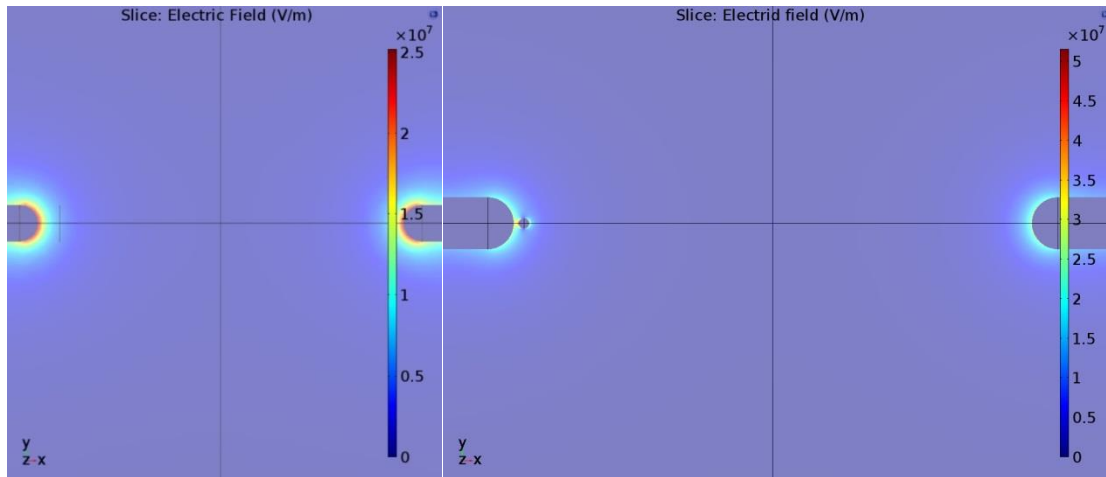


Fig. 16. Electric field without (left) and with 20 μm water droplet (right), 10 μm away from electrode.

3.6.2 Enhancement change with distance between droplet and electrode

Electric field change with distance of droplet from the wire is studied, and the maximum electric field is enhanced more as the $100\mu\text{m}$ -diameter droplet gets closer to the wire (the mesh are much coarser in this case), with the results are shown in Fig. 17. The maximum electric field strength is about 3×10^7 V/m when the particle is $50\mu\text{m}$ away from the wire, which is close to the case without droplet. At $1\mu\text{m}$ away, the maximum electric field is up to 4.7×10^8 V/m. Therefore, spark is likely to be triggered as the droplet gets closer to the electrode.

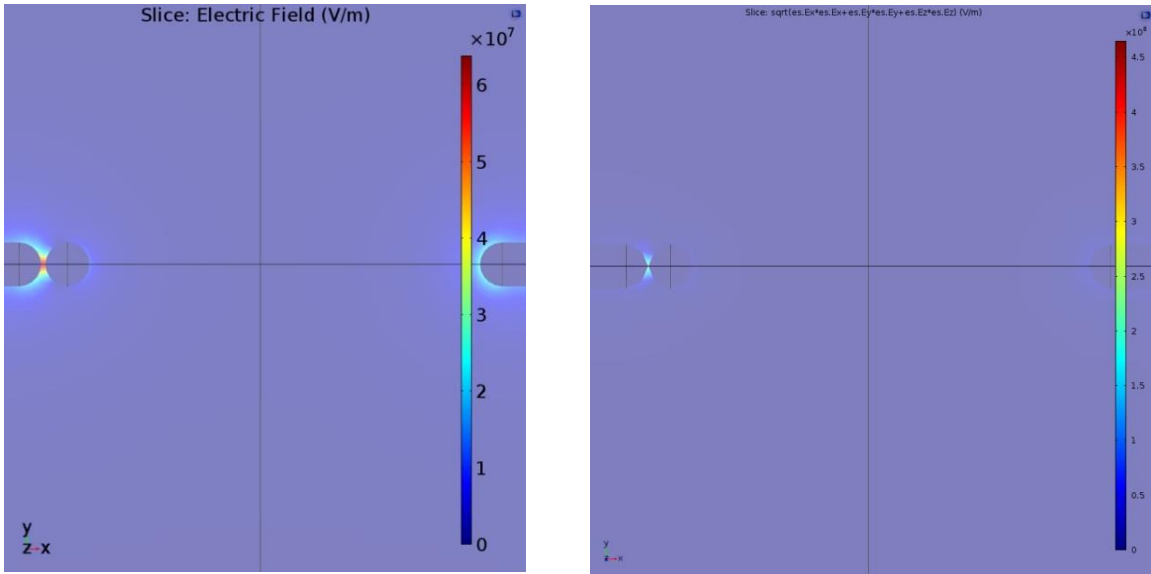


Fig. 17. Electric field with 100 μm water droplet 10 μm (left) and 1 μm (right) away from electrode.

3.6.3 Enhancement change with droplet size

The electric field along the axis between electrodes, for droplets of different sizes, is shown in Fig. 18. The size of the droplet varies from 10 μm to 980 μm , with a constant distance of 10 μm between the droplet and the electrode. The max electric field strength existing in the small gap (from -500 to -490 μm in the figure) between the electrode and the droplet increases with droplet size. However, the max electric field strength on the right side of the droplet decreases as the size of the droplet increases. Furthermore, on the other side, the initial ions are also blocked by the presence of a large droplet, and the combined effect determines if a spark will be initiated.

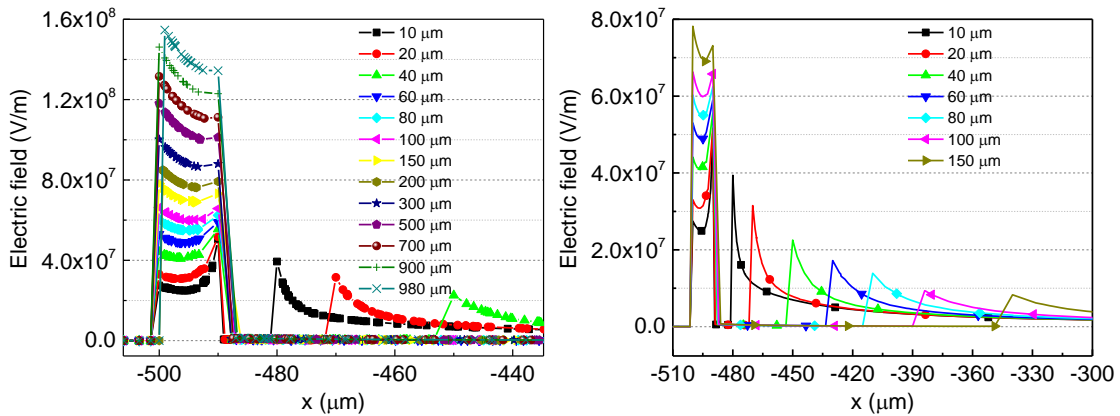
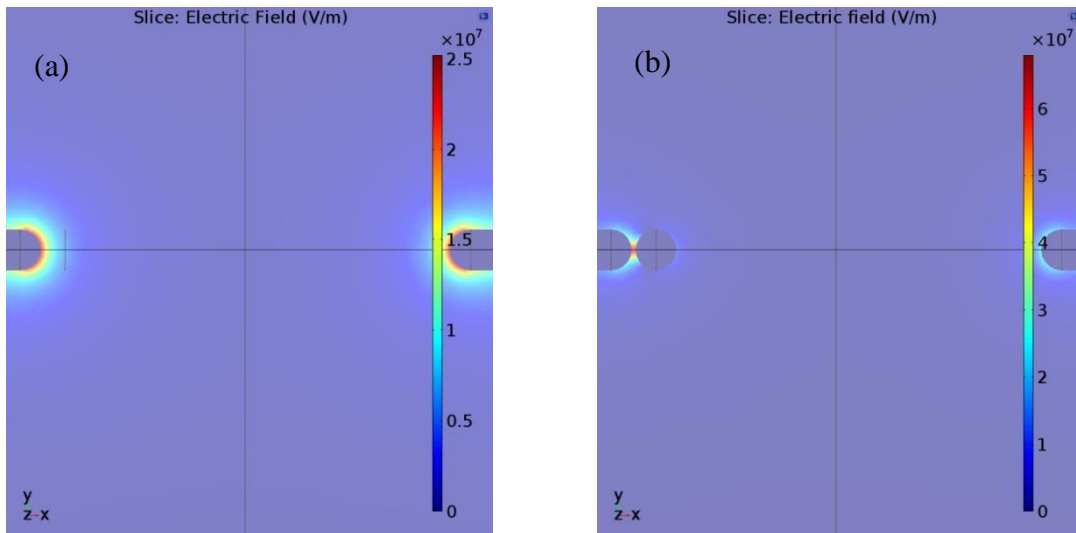


Fig. 18. Electric field with water droplets of different size.

3.6.4 Enhancement change with different liquid

The different behaviors with water, methanol, and toluene are also studied with COMSOL simulation. The dielectric constants are 1, 80, 32.7, and 2.38, for air, water, methanol, and toluene, respectively. The electric field strengths for all cases are plotted in Fig. 19. The maximum electric field strengths are $2.5 \times 10^7 \text{V/m}$, $7 \times 10^7 \text{V/m}$, $6.5 \times 10^7 \text{V/m}$, and $3.7 \times 10^7 \text{V/m}$ for air, water, methanol, and toluene, respectively. The enhancement factor of the electric field depends on the dielectric constant of the materials in-between the electrodes. With high dielectric constant, such as water and methanol, the electric field is greatly enhanced, and sparks can be triggered with the presence of such droplets. However, for materials with the low dielectric constant, such as toluene, the enhancement factor is not large enough. Furthermore, with quenching of the initial ions on the surface of the droplets, the total effect could actually increase the spark threshold. The simulation results are consistent with the experiments, giving insight into the mechanism for triggering of the spark.



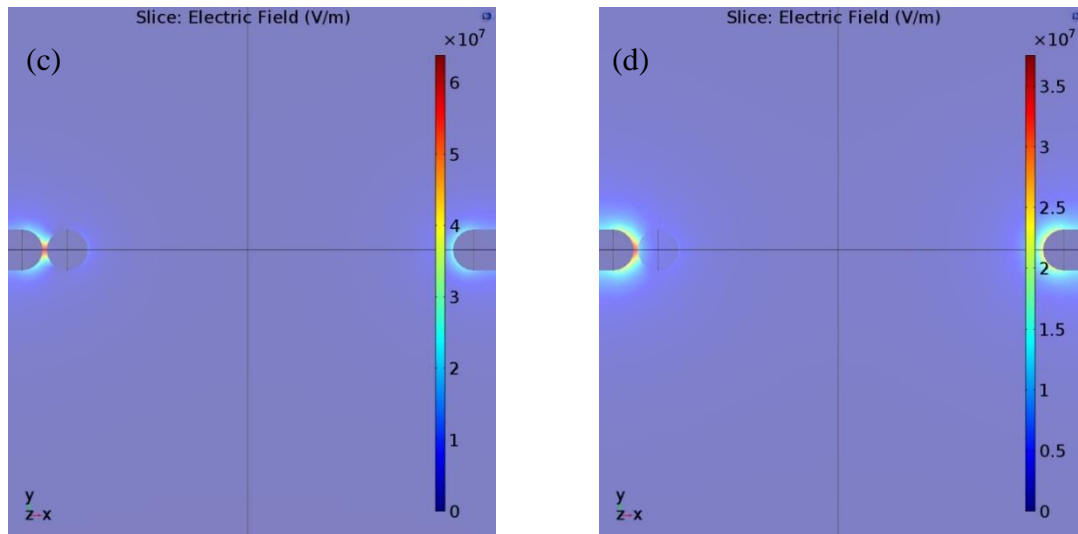


Fig. 19. Electric field around the electrode (a) without droplet, and with a 100 μm droplet 10 μm away from electrode composed of (b) water, (c) methanol, and (d) toluene.

4 Conclusions

In this project, electric breakdown triggered by the presence of non-conductive droplets is studied with experiment and simulation. The presence of droplets can lower the threshold for breakdown by a large extent. There are several modes to trigger spark by the presence of droplets: (1) electrospray from the deposited liquid on the electrode; (2) single droplet repelled from the deposited liquid moving toward the opposite electrode; (3) single droplet attracted to an electrode but then forming an electrospray; and (4) presence of a single droplet very close to an electrode. The mechanism for triggering of the spark is attributed to electric field enhanced by the presence of high dielectric-constant liquid. The presence of materials in-between the electrode may also hinder the spark because of the adhesion of the initial ions onto the surfaces of the droplets or particles.

References

- [1] E. Randeberg, R.K. Eckhoff, Initiation of dust explosions by electric spark discharges triggered by the explosive dust cloud itself, *Journal of Loss Prevention in the Process Industries*. 19 (2006) 154–160. doi:10.1016/j.jlp.2005.05.003.
- [2] G. Kumar, J. Amarnath, B. Singh, K. Srivastava, Particle initiated discharges in gas insulated substations by random movement of particles in electromagnetic fields, *INTERNATIONAL JOURNAL OF APPLIED ELECTROMAGNETICS AND MECHANICS*. 29 (2009) 117–129.
- [3] L. Dascalescu, A. Samuila, R. Tobazéon, Dielectric behaviour of particle-contaminated air-gaps in the presence of corona, *Journal of Electrostatics*. 36 (1996) 253–275. doi:10.1016/0304-3886(95)00050-X.

- [4] J.R. Laghari, A.H. Qureshi, A Review of Particle-Contaminated Gas Breakdown, IEEE Transactions on Electrical Insulation. EI-16 (1981) 388–398. doi:10.1109/TEI.1981.298434.
- [5] H. Parekh, K.D. Srivastava, Breakdown Voltage in Particle Contaminated Compressed Gases, IEEE Transactions on Electrical Insulation. EI-14 (1979) 101–106. doi:10.1109/TEI.1979.298162.
- [6] H. Kuwahara, S. Inamura, T. Watanabe, Y. Arahata, Effect of Solid Impurities on Breakdown in Compressed SF₆ Gas, IEEE Transactions on Power Apparatus and Systems. PAS-93 (1974) 1546–1555. doi:10.1109/TPAS.1974.293885.
- [7] U. Riebel, R. Radtke, R. Loos, An experimental investigation on corona quenching, Journal of Electrostatics. 54 (2002) 159–165. doi:10.1016/S0304-3886(01)00175-9.
- [8] Y.G. Stommel, M. Kirchhoff, U. Riebel, Experimental results on the influence of concentrated liquid aerosols on the onset voltage of corona discharge, Journal of Electrostatics. 64 (2006) 836–842. doi:10.1016/j.elstat.2006.02.004.
- [9] P. Tardiveau, E. Marode, Point-to-plane discharge dynamics in the presence of dielectric droplets, J. Phys. D: Appl. Phys. 36 (2003) 1204. doi:10.1088/0022-3727/36/10/309.
- [10] D.-R. Chen, D.Y.H. Pui, S.L. Kaufman, Electrospraying of conducting liquids for monodisperse aerosol generation in the 4 nm to 1.8 μ m diameter range, Journal of Aerosol Science. 26 (1995) 963–977. doi:10.1016/0021-8502(95)00027-A.
- [11] A. Jaworek, A.T. Sobczyk, Electrospraying route to nanotechnology: An overview, Journal of Electrostatics. 66 (2008) 197–219. doi:10.1016/j.elstat.2007.10.001.
- [12] A.A. Fridman, L.A. Kennedy, Plasma physics and engineering, Taylor & Francis, New York, 2004.